Green functions for nearest- and next-nearest-neighbor hopping on the Bethe lattice

M. Kollar[*1], **M. Eckstein**[1], **K. Byczuk**[1,2], **N. Blümer**[3], **P. van Dongen**[3], **M. H. Radke de Cuba**[4], **W. Metzner**[5], **D. Tanasković**[6], **V. Dobrosavljević**[6], **G. Kotliar**[7], and **D. Vollhardt**[1]

[1] Theoretische Physik III, Elektronische Korrelationen und Magnetismus, Institut für Physik, Universität Augsburg, 86135 Augsburg, Germany

[2] Institute of Theoretical Physics, Warsaw University, ul. Hoza 69, 00-681 Warszawa, Poland

[3] Institut für Physik, KOMET 337, Universität Mainz, 55099 Mainz, Germany

[4] Werkstraße 12, 52076 Aachen, Germany

[5] Max-Planck-Institut für Festkörperforschung, Heisenbergstr. 1, 70569 Stuttgart, Germany

[6] Department of Physics and National High Magnetic Field Laboratory, Florida State University, 1800 E. Paul Dirac Drive, Tallahassee, FL 32310-3706, USA

[7] Department of Physics and Astronomy, Rutgers University, PO Box 849, Piscataway, NJ 08854-8019, USA

Dedicated to Bernhard Mühlschlegel on the occasion of his 80th birthday

We calculate the local Green function for a quantum-mechanical particle with hopping between nearest and next-nearest neighbors on the Bethe lattice, where the on-site energies may alternate on sublattices. For infinite connectivity the renormalized perturbation expansion is carried out by counting all non-self-intersecting paths, leading to an implicit equation for the local Green function. By integrating out branches of the Bethe lattice the same equation is obtained from a path integral approach for the partition function. This also provides the local Green function for finite connectivity. Finally, a recently developed topological approach is extended to derive an operator identity which maps the problem onto the case of only nearest-neighbor hopping. We find in particular that hopping between next-nearest neighbors leads to an asymmetric spectrum with additional van-Hove singularities.

1 Introduction

The Bethe lattice plays an important role in statistical mechanics and condensed matter theory. It is defined as an infinite tree graph in which each vertex has Z edges, such that any two vertices are connected by only one shortest path, as shown in Fig. 1. Several physical problems involving interactions and/or disorder can be solved exactly for the Bethe lattice due to its recursive structure, e.g., Ising models [1,2], or Anderson localization [3–6]. Furthermore the Bethe lattice is useful as a model for the electronic structure of amorphous solids [7]; see [8] for a recent application.

In this article we study the spectra of tight-binding Hamiltonians with hopping between nearest (NN) and next-nearest neighbors (NNN) on the Bethe lattice. In this context the standard methods of solid-state

---

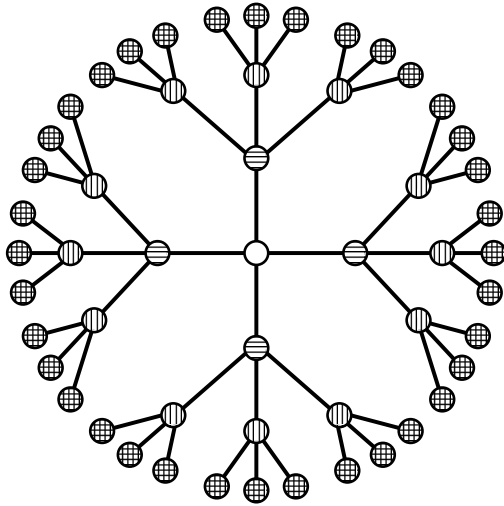 * Corresponding author   E-mail: marcus.kollar@physik.uni-augsburg.de

Fig. 1 Part of the Bethe lattice with coordination number $Z = 4$. Any two sites are connected by a unique shortest path of bonds. Starting from the site marked by the open circle, horizontally shaded circles can be reached by one lattice step (NN), vertically shaded circles by two lattice steps (NNN), and doubly shaded circles by three lattice steps. Note that the lattice is infinite and bipartite.

physics which are based on Bloch's theorem cannot be directly applied. This has led to the development of several alternative approaches to calculate the tight-binding spectrum for NN hopping on the Bethe lattice [9–14]. However, some of these methods become very complicated for hopping beyond NN due to the proliferation of hopping paths. Below we apply and further develop several different calculational schemes to determine the Green function in the presence of both NN and NNN hopping.

In terms of the quantum-mechanical single-particle operator $|i\rangle\langle j|$, which removes a particle from site j and recreates it at site i, the general, translationally invariant hopping Hamiltonian on the Bethe lattice has the form

$$H_{\text{kin}} = \sum_{ij} t_{ij} |i\rangle\langle j| = \sum_{d \geq 0} t_d H_d \,, \qquad\qquad H_d = \sum_{d_{i,j}=d} |i\rangle\langle j| \,. \qquad (1)$$

Here hopping processes between two sites i and j are classified according to their topological distance $d_{i,j}$, i.e., the number of nearest-neighbor steps of the shortest path between i and j. We will also allow for an alternating on-site energy ϵ_i,

$$H_{\text{loc}} = \sum_i \epsilon_i |i\rangle\langle i| \,, \qquad \epsilon_i = \begin{cases} \epsilon_{\text{A}} & \text{if } i \in \text{A} \\ \epsilon_{\text{B}} & \text{if } i \in \text{B} \end{cases} \,, \qquad (2)$$

where ϵ_i depends only on the sublattice $\gamma = \text{A}, \text{B}$ of the bipartite Bethe lattice to which i belongs. In correlated systems, e.g., for the Hubbard model, on-site energies (2) may be used to detect antiferromagnetic symmetry breaking.

A well-defined limit for infinite coordination number Z results if the hopping amplitudes and Hamiltonians are scaled according to [15]

$$t_d = \frac{t_d^*}{K^{d/2}} \,, \qquad\qquad \tilde{H}_d = \frac{H_d}{K^{d/2}} \,, \qquad\qquad t_d H_d = t_d^* \tilde{H}_d \,, \qquad (3)$$

where $K = Z - 1$ is the connectivity. In the limit $K \to \infty$ dynamical mean-field theory (DMFT) [16–21] becomes exact. In particular for the Hubbard model the self-energy is then local in space and may be obtained from a single-impurity problem with self-consistency condition [20]. In recent years DMFT for the Hubbard model on the Bethe lattice has greatly helped to understand the Mott transition from a paramagnetic metal to a paramagnetic insulator at half-filling [16–26]. For the paramagnetic phase to be stable the antiferromagnetic low-temperature phase of the Hubbard model needs to be suppressed by frustration; only then the Mott

transition is observable. This can be achieved by including *random* hopping beyond NN [20, 27–30]. In this case the density of states (DOS) remains semi-elliptic, implying that the Mott transition in the paramagnetic phase is unchanged. On the other hand, for *nonrandom* NNN hopping the DOS is usually asymmetric, and this is also the case for the Bethe lattice [14]. Moreover, an asymmetric DOS is known to stabilize ferromagnetism away from half-filling [31–33].

Here, as a prerequisite for any investigations of frustrated interacting or disordered systems, we will study the noninteracting Hamiltonian with (nonrandom) NN and NNN hopping

$$H = H_{\text{loc}} + t_1 H_1 + t_2 H_2 = H_{\text{loc}} + t_1^* \tilde{H}_1 + t_2^* \tilde{H}_2 \tag{4}$$

and obtain its local Green function $G_i(z)$, defined for $\operatorname{Im} z \neq 0$ by

$$G_{ij}(z) := \langle i | \frac{1}{z-H} | j \rangle , \qquad G_i(z) := G_{ii}(z) , \qquad G_i^\infty(z) := \lim_{K \to \infty} G_i(z) , \tag{5}$$

paying special attention to the limit $K \to \infty$. Note that due to translational symmetry of the infinite Bethe lattice $G_i(z) =: G_\gamma(z)$ depends only on the sublattice γ of i. We recall that for only NN hopping the local Green function for sublattice γ is given by [11]

$$g_\gamma(z) := \langle i | \frac{1}{z-h} | i \rangle = \frac{2K(z - \epsilon_{\bar{\gamma}})}{(K-1)x + (K+1)\sqrt{x - 4t_1^{*2}}\sqrt{x}} , \qquad h = H_{\text{loc}} + t_1^* \tilde{H}_1 , \tag{6}$$

where $x = (z - \epsilon_{\text{A}})(z - \epsilon_{\text{B}})$ and the square roots are given by their principal branches.

The derivation of the local Green function for t_1-t_2 hopping will proceed as follows. In Sect. 2 we use the renormalized perturbation expansion (RPE) [11] to obtain a closed set of equations for $G_\gamma^\infty(z)$, which are also related to the DMFT selfconsistency equations. The RPE method is well-suited for the Bethe lattice due to its recursive nature, although the classification of paths for $t_2 \neq 0$ is rather involved. We show how to use the RPE result to establish the asymmetry of the DOS. On the other hand, in Sect. 3 we use the many-body path integral approach [34] to derive an exact effective action by a recursive method. This also yields closed equations for the local Green functions $G_\gamma(z)$ for any coordination number Z. Furthermore a surprising algebraic relation between Green functions for finite and infinite Z is uncovered. Finally, in Sect. 4 a recently developed topological method [14] is extended to include H_{loc}. We derive an operator identity, valid for any Z, that allows one to express $G_\gamma(z)$ in terms of the known solutions (6) for only NN hopping. Our results for the local Green function are discussed in Sect. 5. A conclusion in Sect. 6 closes the presentation.

2 Renormalized perturbation expansion

2.1 Dressed expansion for the local Green function

In this section we obtain an equation for the local Green function (5) using the renormalized perturbation expansion (RPE) [11, 35]. In this approach the Green function $G_{ij}(z)$ for H is obtained in terms of the Green function $G_{ij}^{\text{loc}}(z) = \delta_{ij} G_i^{\text{loc}}(z)$ for H_{loc} as

$$G_{ij} = \delta_{ij} G_i^{\text{loc}} + G_i^{\text{loc}} t_{ij} G_j^{\text{loc}} + \sum_k G_i^{\text{loc}} t_{ik} G_k^{\text{loc}} t_{kj} G_j^{\text{loc}} + \cdots , \qquad G_i^{\text{loc}} = \frac{1}{z - \epsilon_i} , \tag{7}$$

where we omit the argument z for the moment. This expansion contains terms in which site indices are repeated. In a graphical representation this corresponds to paths in which some lattice sites are "decorated" with closed paths [11]. One can omit these decorations at the first site i by replacing G_i^{loc} by the full local Green function G_i. At the next site k, however, the decorations at site i must not be repeated, leading to the

replacement of G_k^{loc} by the local Green function with site i removed, i.e., by $G_k^{[i]} = G_k|_{\epsilon_i=\infty}$. Repeating this process one obtains

$$G_i = G_i^{\text{loc}} + \sum_k{}' G_i\, t_{ik}\, G_k^{[i]}\, t_{ki}\, G_i^{\text{loc}} + \sum_{km}{}' G_i\, t_{ik}\, G_k^{[i]}\, t_{km}\, G_m^{[i,k]}\, t_{mi}\, G_i^{\text{loc}} + \cdots, \tag{8}$$

where the primed sums are now only over non-self-intersecting paths. The RPE is particularly useful in the limit $Z \to \infty$ which allows the replacement $G_i^{[\cdots]} \to G_i^\infty$. This yields an equation involving only local Green functions,

$$G_i^\infty(z)^{-1} = z - \epsilon_i - \left[\sum_k t_{ik}\, G_k^\infty(z)\, t_{ki} + \sum_{km}{}' t_{ik}\, G_k^\infty(z)\, t_{km}\, G_m^\infty(z)\, t_{mi} + \cdots \right]. \tag{9}$$

For the case of two sublattices with on-site energies ϵ_A, ϵ_B we thus obtain two coupled equations ($\gamma = A,B$; $\bar{A} = B$, $\bar{B} = A$),

$$G_\gamma^\infty(z)^{-1} = z - \epsilon_\gamma - F(G_\gamma^\infty(z), G_{\bar\gamma}^\infty(z)). \tag{10}$$

This is a closed system of implicit equations for the local Green functions $G_\gamma^\infty(z)$.

Note that the self-consistency equations of DMFT are essentially contained in Eq. (10). In DMFT the self-energy is local [20], $\Sigma_{ij}(z) = \Sigma_\gamma(z)\delta_{ij}$ for $i \in \gamma$, and the local *interacting* Green function $G_\gamma^{\text{int}}(z)$ is given by the Dyson equation $G_\gamma^{\text{int}}(z)^{-1} = G_\gamma^\infty(z - \Sigma_\gamma(z))^{-1} = \mathcal{G}_\gamma(z)^{-1} - \Sigma_\gamma(z)$, where $\mathcal{G}_\gamma(z)$ is the Weiss field of an auxiliary single-site problem for sublattice γ. From Eq. (10) one thus obtains the self-consistency equation

$$\mathcal{G}_\gamma(z)^{-1} = z - \epsilon_\gamma - F(G_\gamma^{\text{int}}(z), G_{\bar\gamma}^{\text{int}}(z)). \tag{11}$$

Here spin indices were suppressed for simplicity. Detailed discussions of DMFT self-consistency equations can be found in Refs. [14, 20].

2.2 RPE for t_1-t_2 hopping on the Bethe lattice

For the remainder of this section we consider the Bethe lattice in the limit $Z \to \infty$. As a standard example, we first consider only NN hopping (6). Since no closed loops are possible, the only allowed non-self-intersecting paths are visits to one of the Z NN sites which return immediately. This yields the well-known equation [11]

$$g_\gamma^\infty(z)^{-1} = z - \epsilon_\gamma - t_1^{*2}\, g_{\bar\gamma}^\infty(z), \qquad g_\gamma^\infty(z) = \frac{2(z - \epsilon_{\bar\gamma})}{x + \sqrt{x - 4t_1^{*2}}\sqrt{x}}, \qquad (t_2 = 0) \tag{12}$$

where the solution is a special case of Eq. (6).

We now proceed to the case of t_1-t_2 hopping, for which the evaluation of the square bracket in Eq. (9) is more involved, since it requires the enumeration [26, 36] of several classes of closed non-self-intersecting paths which begin and end at site i. First we note that at each site j ($\neq i$) on the path it is possible to make a detour within the same shell, i.e., to one of the yet unvisited NNN sites k of j with same distance $d_{i,j} = d_{i,k}$ from i, as illustrated in Fig. 2a. In the limit $Z \to \infty$ we can take these detours into account by replacing G_γ^∞ by

$$\widehat{G}_\gamma^\infty = G_\gamma^\infty + G_\gamma^\infty\, t_2^*\, G_\gamma^\infty + G_\gamma^\infty\, t_2^*\, G_\gamma^\infty\, t_2^*\, G_\gamma^\infty + \cdots = \frac{G_\gamma^\infty}{1 - t_2^*\, G_\gamma^\infty} \tag{13}$$

and only considering non-self-intersecting paths that *change shells in every step*. Such shell-changing, non-self-intersecting paths are referred to as *proper paths* from now on. They may be drawn using simplified
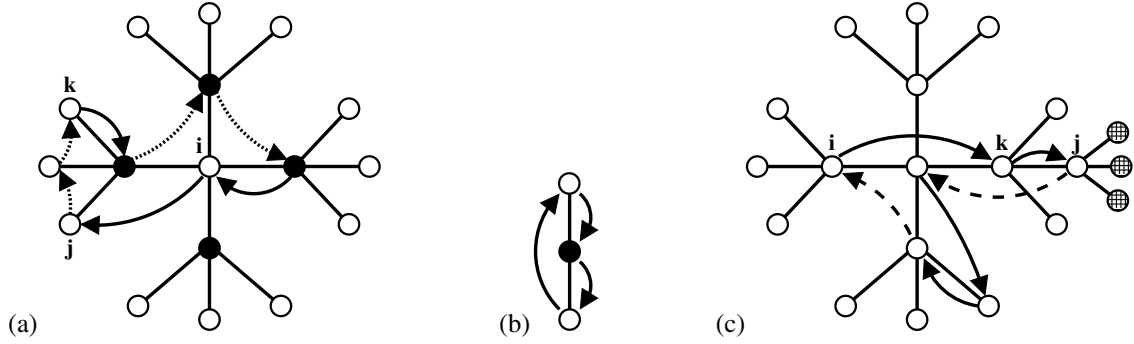
Fig. 2 (a) Example of intra-shell detours in RPE. A non-self-intersecting path, which starts and ends at site i, may contain NNN steps (dotted) to sites with the same distance from i, e.g., from j to k. Open and solid circles indicate γ and $\bar{\gamma}$ sublattices. (b) Simplified diagram for the proper path corresponding to (a). (c) Rule (14) for proper paths: After visiting k and j, the shaded sites are blocked and one must return towards i. From a NN site of i it may then either return immediately to i or leave again with NNN steps, eventually taking a NN step and being forced back to i. Dashed arrows indicate forced moves.

diagrams indicating the visited shells only, see Fig. 2b. Closed proper paths, starting and ending at site i, are then governed by the following rule:

Whenever two neighboring sites j and k have been visited, with j further away (14)
from i than k, all sites on j's branch further away from i than j cannot be visited.

This rule, which is illustrated in Fig. 2c, is due to the tree-like structure of the Bethe lattice and the requirements that the paths are non-self-intersecting, involve only NN or NNN steps, and change shells in every step. It is not affected by intra-shell detours contained in $\widehat{G}_\gamma^\infty$.

Therefore a sequence of outgoing NNN steps, starting at a site in shell 0 or 1 and terminated by a NN step *must* be followed by a NNN step going inward until shell 1 or 0, respectively, is reached. We are thus led to the following classification of proper paths by their outermost shell $s_{\max}$, as shown in Fig. 3 and listed in Table 1:

(a) An even shell $s_{\max}$ is reached by taking NNN steps. After taking one NN step inward the path must return towards i until reaching shell 1 due to rule (14). Then the path may turn outward again, finally using a NN step (a1) inward or (a2) outward to reach i's sublattice and return. The reverse path is also possible, but in case (a1) may be identical.

(b) An odd shell $s_{\max}$ is reached by taking NNN steps and one NN step outward. After returning to shell 1 due to rule (14), one may turn outward again in (b1) and (b2) similar to (a1) and (a2). The reverse path is also possible, but in case (b2) may be identical.

(c) Whereas (a) and (b) involve at least one NN step, there is also one proper path involving no NN step; it visits a NNN site and returns immediately.

Note that paths that start with a NN step are included in the inverted paths mentioned under (a) and (b). The contributions of all proper paths are also collected in Table 1, and their sum is

$$F(G_\gamma^\infty, G_{\bar{\gamma}}^\infty) = \sum_{m=1}^\infty \sum_{k=0}^{m-1} \left[G_{\gamma,m,k}^{(a1)} + G_{\gamma,m,k}^{(a2)} \right] + \sum_{m=0}^\infty \sum_{k=0}^m \left[G_{\gamma,m,k}^{(b1)} + G_{\gamma,m,k}^{(b2)} \right] + G_\gamma^{(c)}$$

$$= \frac{t_1^{*2} G_{\bar{\gamma}}^\infty (1 - t_2^* G_{\bar{\gamma}}^\infty)}{(1 - t_2^* G_\gamma^\infty - t_2^* G_{\bar{\gamma}}^\infty)^2} + \frac{t_2^{*2} G_\gamma^\infty}{1 - t_2^* G_\gamma^\infty}. \tag{15}$$

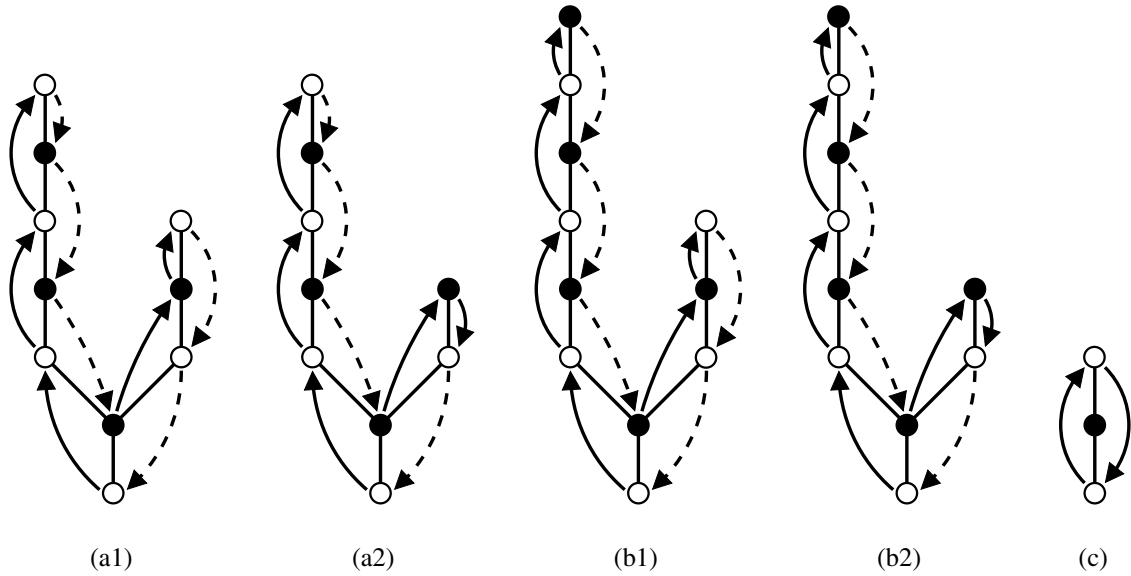|				
(a1)	(a2)	(b1)	(b2)	(c)

Fig. 3 Simplified diagrams for proper paths that contribute to Eq. (15). Only paths which change the shell in each step are considered; the effect of intra-shell detours is taken into account by working with dressed Green functions $\widehat{G}_\gamma^\infty$, $\widehat{G}_{\bar\gamma}^\infty$. Open and solid circles indicate γ and $\bar\gamma$ sublattices, respectively. Dashed arrows indicate moves that are forced due to the rules (14). See Table 1 for details.

Eqs. (10) and (15) are a set of coupled quartic equations for G_γ^∞ and $G_{\bar\gamma}^\infty$. Eq. (15), taken together with (11), fully determines the DMFT self-consistency equation for t_1-t_2 hopping on the Bethe lattice. This result differs [14, 36] from the self-consistency equations employed in Refs. [20, 27–30], which apply only to random hopping.

The result (15) can immediately be used to determine the moments M_n of the density of states. For the case $\epsilon_A = \epsilon_B = 0$ we have the large-z expansion

$$G_\gamma^\infty(z) = \int\limits_{-\infty}^{\infty} \frac{\rho^\infty(\epsilon)}{z - \epsilon}\, d\epsilon =: \sum_{n=0}^{\infty} \frac{M_n}{z^{n+1}}\,, \qquad \rho^\infty(\epsilon) := -\frac{1}{\pi}\mathrm{Im}\, G_\gamma^\infty(\epsilon + i0)\,. \qquad (16)$$

Multiplying Eq. (10) by G_γ^∞, inserting Eq. (16), and comparing coefficients of powers of z we find

$$M_1 = 0\,, \quad M_2 = t_1^{*2} + t_2^{*2}\,, \quad M_3 = (3t_1^{*2} + t_2^{*2})\, t_2^*\,, \quad M_4 = 2t_1^{*4} + 12t_1^{*2}t_2^{*2} + 3t_2^{*4}\,, \quad (17)$$

revealing at once that the DOS $\rho^\infty(\epsilon)$ is asymmetric for $t_2^* \neq 0$ [26], in contrast to the case of random hopping [20, 27–30].

Clearly the RPE is well-suited for the Bethe lattice because rule (14) represents a strict constraint on proper paths. However, already for the case of t_1-t_2 hopping the RPE requires some care. Furthermore, the enumeration of paths for hopping *beyond NNN*, or for $Z < \infty$, is likely to be very tedious. Another drawback is that the RPE only yields an implicit system of equations for the local Green functions. Below we derive explicit expressions for them via a different route.

Table 1 Proper paths contributing to Eq. (15) for a Bethe lattice with $Z \to \infty$. Paths (a1) and (a2) reach an even outermost shell, while paths (b1) and (b2) reach an odd outermost shell; both contain at least one NN step. On the other hand, without NN steps only path (c) is possible. Steps forced by rule (14) are marked by an asterisk (*). The reversion of each non-symmetric path yields a factor of 2.

	path	steps	factor	reached shell
(a)	$s_{\max} = 2m$	1. m NNN steps outward	$(t_2^*)^m (\widehat{G}_\gamma^\infty)^m$	$2m$
	$(m \geq 1)$	2. 1 NN step inward	$(t_1^*)(\widehat{G}_{\overline{\gamma}}^\infty)$	$2m-1$
		3. $(m-1)$ NNN steps inward*	$(t_2^*)^{m-1}(\widehat{G}_{\overline{\gamma}}^\infty)^{m-1}$	1
		4. k NNN steps outward $(k \leq m-1)$	$(t_2^*)^k (\widehat{G}_{\overline{\gamma}}^\infty)^k$	$2k+1$
(a1)		5. 1 NN step outward	$(t_1^*)(\widehat{G}_\gamma^\infty)$	$2k+2$
		6. $(k+1)$ NNN steps inward*	$(t_2^*)^{k+1}(\widehat{G}_\gamma^\infty)^k$	0
		reverse path (if different)	$(2 - \delta_{k,m-1})$	

$$G_{\gamma,m,k}^{(a1)} = (2 - \delta_{k,m-1})(t_1^*)^2 (t_2^*)^{2m+2k}(\widehat{G}_\gamma^\infty)^{m+k+1}(\widehat{G}_{\overline{\gamma}}^\infty)^{m+k}$$

	path	steps	factor	reached shell
(a2)		5. 1 NN step inward	$(t_1^*)(\widehat{G}_\gamma^\infty)$	$2k$
		6. k NNN steps inward*	$(t_2^*)^k (\widehat{G}_\gamma^\infty)^{k-1}$	0
		reverse path	2	

$$G_{\gamma,m,k}^{(a2)} = 2(t_1^*)^2 (t_2^*)^{2m+2k-1}(\widehat{G}_\gamma^\infty)^{m+k}(\widehat{G}_{\overline{\gamma}}^\infty)^{m+k}$$

	path	steps	factor	reached shell
(b)	$s_{\max} = 2m+1$	1. m NNN steps outward	$(t_2^*)^m (\widehat{G}_\gamma^\infty)^m$	$2m$
	$(m \geq 0)$	2. 1 NN step outward	$(t_1^*)(\widehat{G}_{\overline{\gamma}}^\infty)$	$2m+1$
		3. m NNN steps inward*	$(t_2^*)^m (\widehat{G}_{\overline{\gamma}}^\infty)^m$	1
		4. k NNN steps outward $(k \leq m)$	$(t_2^*)^k (\widehat{G}_{\overline{\gamma}}^\infty)^k$	$2k+1$
(b1)		5. 1 NN step outward (if $k \neq m$)	$(t_1^*)(\widehat{G}_\gamma^\infty)$	$2k+2$
		6. $(k+1)$ NNN steps inward*	$(t_2^*)^{k+1}(\widehat{G}_\gamma^\infty)^k$	0
		reverse path	2	

$$G_{\gamma,m,k}^{(b1)} = 2(1 - \delta_{k,m})(t_1^*)^2 (t_2^*)^{2m+2k+1}(\widehat{G}_\gamma^\infty)^{m+k+1}(\widehat{G}_{\overline{\gamma}}^\infty)^{m+k+1}$$

	path	steps	factor	reached shell
(b2)		5. 1 NN step inward	$(t_1^*)(\widehat{G}_\gamma^\infty)$	$2k$
		6. k NNN steps inward*	$(t_2^*)^k (\widehat{G}_\gamma^\infty)^{k-1}$	0
		reverse path (if different)	$(2 - \delta_{k,m})$	

$$G_{\gamma,m,k}^{(b2)} = (2 - \delta_{k,m})(t_1^*)^2 (t_2^*)^{2m+2k}(\widehat{G}_\gamma^\infty)^{m+k}(\widehat{G}_{\overline{\gamma}}^\infty)^{m+k+1}$$

	path	steps	factor	reached shell
(c)	$s_{\max} = 2$	1. 1 NNN step outward	$(t_2^*)(\widehat{G}_\gamma^\infty)$	2
	(no NN steps)	2. 1 NN step inward	(t_2^*)	0

$$G_\gamma^{(c)} = (t_2^*)^2 (\widehat{G}_\gamma^\infty)$$

3 Path-integral approach

3.1 Green function as path integral

In this section we use the standard many-body path-integral approach to the local Green function. For non-interacting spinless fermions with Hamiltonian $H_{\mathrm{loc}} + H_{\mathrm{kin}}$ the action is [34]

$$S = \int_0^{1/T} \sum_{ij} \bar{c}_i(\tau) \left[(\partial_\tau - \mu + \epsilon_i)\delta_{ij} + t_{ij} \right] c_j(\tau)\, d\tau \,, \tag{18}$$

where $\bar{c}_i(\tau)$, $c_i(\tau)$ are Grassmann variables. Fourier transforming to fermionic Matsubara frequencies, $\omega_n = (2n+1)\pi T$, we obtain $S = \sum_n \sum_{ij} \left[t_{ij} + (\epsilon_i - \mathrm{i}\omega_n - \mu)\delta_{ij} \right] \bar{c}_{in} c_{jn}$, i.e., the functional integral factorizes with respect to n. We thus consider a fixed Matsubara frequency, set $z = \mathrm{i}\omega_n + \mu$, and omit the index n. The local Green function is then given by

$$G_i(z) = \int \prod_j \mathcal{D}[\bar{c}_j, c_j]\, e^{-\tilde{S}}\, \bar{c}_i c_i \, \Big/ \, \int \prod_j \mathcal{D}[\bar{c}_j, c_j]\, e^{-\tilde{S}} \,, \tag{19}$$

with $\tilde{S} = \sum_i S_{\mathrm{loc}}(i) + \frac{1}{2}\sum_{ij} S_{\mathrm{hop}}(i,j)$, $S_{\mathrm{loc}}(i) = -(z - \epsilon_i)\bar{c}_i c_i$, $S_{\mathrm{hop}}(i,j) = t_{ij}(\bar{c}_i c_j + \bar{c}_j c_i)$. Note that for this non-interacting system the many-body Matsubara Green function is independent of the temperature T and coincides with the Green function defined in Eq. (5).

3.2 Decomposition of the action for t_1-t_2 hopping on the Bethe lattice

We now consider t_1-t_2 hopping on the Bethe lattice as in Eq. (4). In this case the following decomposition of the Bethe lattice turns out to be useful. For two NN sites i and j we let $\mathcal{Z}(i|j)$ denote the set of NN sites of i, but with site j omitted. Furthermore $\mathcal{B}(i|j)$ shall denote the sites on all the branches which begin at the sites in $\mathcal{Z}(i|j)$ and lead away from i. These definitions are illustrated in Fig. 4a.

Now consider a partial trace where we integrate out the Grassmann variables for the sites in $\mathcal{B}(i|j)$, i.e., all the sites connected to i except for those on the branch starting at j. We thus define, for NN sites i and j,

$$\Xi(i|j) = \int \prod_{k \in \mathcal{B}(i|j)} \mathcal{D}[\bar{c}_k, c_k]\ \ e^{-S(i|j)} \,, \tag{20}$$
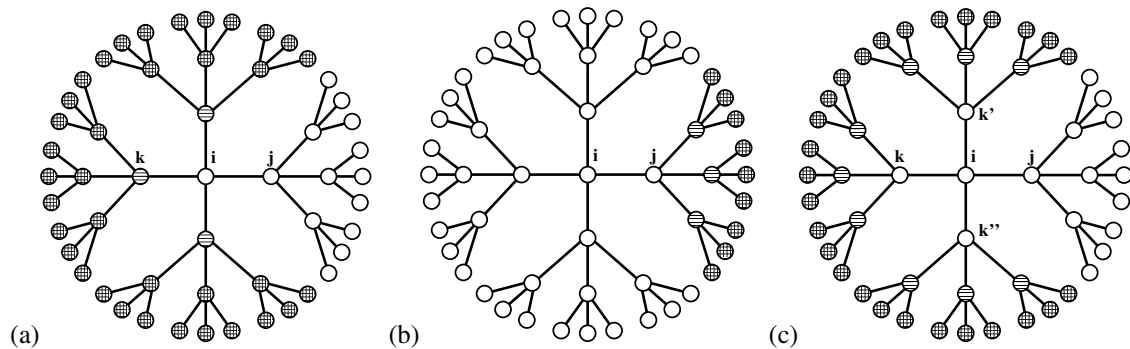

Fig. 4   (a) The NN sites of i, except j, are denoted by $\mathcal{Z}(i|j)$, marked by horizontal shading. $\mathcal{B}(i|j)$ denotes the sites on the branches starting on any $k \in \mathcal{Z}(i|j)$ and leading away from i, marked by horizontal or double shading. $\Xi(i|j)$ [Eq. (20)] involves a trace over shaded sites. (b) Here the shaded sites are involved in the trace appearing in $\Xi(j|i)$ [Eq. (20)]. When combined with the sites traced over in $\Xi(i|j)$, i.e., the shaded sites in (a), one obtains a trace over all sites except i and j, leading to the expression for the local Green function G_i in Eq. (23). (c) The shaded sites in (a) can also be enumerated by combining $\mathcal{B}(k|i)$ for all $k \in \mathcal{Z}(i|j)$, leading to Eq. (25) which expresses $\Xi(i|j)$ in terms of a product $\Xi(k|i)\Xi(k'|i)\cdots$.

$$S(i|j) = \sum_{k \in \mathcal{B}(i|j)} \left[S_{\text{loc}}(k) + S_{\text{hop}}(k,i) + S_{\text{hop}}(k,j) \right] + \frac{1}{2} \sum_{k,m \in \mathcal{B}(i|j)} S_{\text{hop}}(k,m) \,, \tag{21}$$

i.e., we include only the part $S(i|j)$ of the action in the trace that involves Grassmann variables on the branches $\mathcal{B}(i|j)$. As a consequence, the only Grassmann variables remaining in $\Xi(i|j)$ are $\bar{c}_i, c_i$ and $\bar{c}_j, c_j$. Because they are connected to other $\bar{c}_k, c_k$ in $S(i|j)$ only linearly, $\Xi(i|j)$ is of Gaussian form,

$$\Xi(i|j) \propto \exp\left(-\left(\bar{c}_i\ \bar{c}_j\right) \boldsymbol{X}_\gamma \left(\begin{array}{c} c_i \\ c_j \end{array}\right) \right) \,, \qquad\qquad \boldsymbol{X}_\gamma = \left(\begin{array}{cc} u_\gamma & w_\gamma \\ \overline{w}_\gamma & v_\gamma \end{array}\right) \,, \tag{22}$$

for $i \in \gamma$, $j \in \bar{\gamma}$. Here the coefficients in the exponent depend only on the sublattices to which i and j belong, due to the translational invariance of the infinite Bethe lattice. These coefficients will be determined below.

The partial trace in Eq. (20) serves two purposes. On the one hand the local Green function (19) can now be written as a trace over i and a neighboring site j, together with their respective partial traces and the remaining parts of the action,

$$G_i(z) = \frac{\int \mathcal{D}[\bar{c}_i, c_i, \bar{c}_j, c_j] \, \Xi(i|j) \, \Xi(j|i) \, e^{-S_{\text{loc}}(i) - S_{\text{loc}}(j) - S_{\text{hop}}(i,j)} \, \bar{c}_i c_i}{\int \mathcal{D}[\bar{c}_i, c_i, \bar{c}_j, c_j] \, \Xi(i|j) \, \Xi(j|i) \, e^{-S_{\text{loc}}(i) - S_{\text{loc}}(j) - S_{\text{hop}}(i,j)}} \,. \tag{23}$$

This equals (19) because, when considering the two neighboring sites i and j, $\Xi(i|j)$ contains the contributions of all the sites "behind" i, whereas $\Xi(j|i)$ contains the contributions of all the sites "behind" j, as illustrated in Figs. 4a and 4b, and the remaining action involves only i and j because the hopping is only between NN or NNN sites. We note in passing that a generalization to hopping *beyond NNN*, while possible in principle, will become increasingly complicated. Inserting Eq. (22) into (23) gives a Gaussian integral which can be performed by completing the square, yielding

$$G_\gamma(z) = \frac{z_{\bar{\gamma}} - u_{\bar{\gamma}} - v_\gamma}{(z_\gamma - u_\gamma - v_{\bar{\gamma}})(z_{\bar{\gamma}} - u_{\bar{\gamma}} - v_\gamma) - (t_1 + w_{\bar{\gamma}} + \overline{w}_\gamma)(t_1 + w_\gamma + \overline{w}_{\bar{\gamma}})} \tag{24}$$

for the local Green function on sublattice γ, with $z_\gamma = z - \epsilon_\gamma$.

On the other hand one can obtain a functional equation for $\Xi(i|j)$ by decomposing the Bethe lattice in different ways. Recall that $\Xi(i|j)$ contains the branches which start at the NN sites k of i, where $k \neq j$. We can also move one site away from i and consider $\Xi(k|i)$, which contains the branches which start at k's NN neighbors, except i, as illustrated in Fig. 4c. We recover $\Xi(i|j)$ when we multiply the $\Xi(k|i)$'s, include pieces of the action which connect the $\mathcal{B}(k|i)$ among each other and with i and j, and trace over the sites k. Thus we arrive at

$$\Xi(i|j) = \int \prod_{k \in \mathcal{Z}(i|j)} \mathcal{D}[\bar{c}_k, c_k] \prod_{k \in \mathcal{Z}(i|j)} \Xi(k|i)$$

$$\times \exp\left(-\sum_{k \in \mathcal{Z}(i|j)} \left[S_{\text{loc}}(k) + S_{\text{hop}}(k,i) + S_{\text{hop}}(k,j) + \frac{1}{2} \sum_{k'(\neq k) \in \mathcal{Z}(i|j)} S_{\text{hop}}(k,k') \right] \right) , \tag{25}$$

where i and j are any two NN sites.

Now $\Xi(i|j)$ can be determined from the above relation, using its Gaussian form (22). Due to the translational symmetry of the infinite Bethe lattice it suffices to consider, say, $i = 0 \in \gamma$ and $j = 1 \in \bar{\gamma}$. From Eqs. (22) and (25) we then obtain

$$\Xi(0|1) \propto \int \prod_{k=2}^{Z} \mathcal{D}[\bar{c}_k, c_k] \exp\left(-K \bar{c}_0 v_{\bar{\gamma}} c_0 - \sum_{i=2}^{Z} (\bar{\xi} c_i + \bar{c}_i \xi) - \sum_{i,j=2}^{Z} \bar{c}_i M_{ij} c_j \right) , \tag{26}$$

where $K = Z - 1$, $\overline{\xi} = (t_1 + \overline{w}_{\overline{\gamma}})\overline{c}_0 + t_2\overline{c}_1$, $\xi = (t_1 + w_{\overline{\gamma}})c_0 + t_2 c_1$, and the product and sums are over nearest neighbors of site 0 other than site 1. The $K \times K$ matrix $\boldsymbol{M}$ in the Gaussian integral and its inverse are of the form $M_{ij} = \delta_{ij} a + (1 - \delta_{ij}) b$ and $(\boldsymbol{M}^{-1})_{ij} = \delta_{ij} c + (1 - \delta_{ij}) d$, respectively, with $c = (a + (K - 2)b)/q$, $d = -b/q$, and $q = a^2 + (K - 2)ab - (K - 1)b^2$. Here $a = u_{\overline{\gamma}} - z_{\overline{\gamma}}$ and $b = t_2$. The Gaussian integration in Eq. (26) is performed by completing the square, yielding

$$\Xi(0|1) \propto \exp\left(-K\,\overline{c}_0 v_{\overline{\gamma}} c_0 - \overline{\xi}\xi \sum_{i,j=2}^{Z} (\boldsymbol{M}^{-1})_{ij}\right) = \exp\left(-K\overline{c}_0 v_{\overline{\gamma}} c_0 - K\overline{\xi}\frac{a - b}{q}\xi\right). \quad (27)$$

Comparing with Eq. (22) we thus obtain the following system of equations:

$$u_{\gamma} = K\,v_{\overline{\gamma}} + K\,(t_1 + \overline{w}_{\overline{\gamma}})\,(t_1 + w_{\overline{\gamma}})\,\widehat{G}_{\overline{\gamma}}\,, \quad (28)$$

$$w_{\gamma} = K\,t_2\,(t_1 + \overline{w}_{\overline{\gamma}})\,\widehat{G}_{\overline{\gamma}}\,, \quad (29)$$

$$\overline{w}_{\gamma} = K\,t_2\,(t_1 + w_{\overline{\gamma}})\,\widehat{G}_{\overline{\gamma}}\,, \quad (30)$$

$$v_{\gamma} = K\,t_2^2\,\widehat{G}_{\overline{\gamma}}\,, \quad (31)$$

with the abbreviation $\widehat{G}_{\gamma} = [z_{\gamma} - u_{\gamma} - (K - 1)t_2]^{-1}$.

3.3 Local Green function for arbitrary connectivity

For easier discussion of the limit $Z \to \infty$ we use the scaled hopping parameters of Eq. (3). Putting $\tilde{z} = z + t_2^*/K$ and $\widetilde{G}_{\gamma} = \widehat{G}_{\gamma}/(1 + t_2^*\widehat{G}_{\gamma}) = (\tilde{z} - \epsilon_{\gamma} - u_{\gamma})^{-1}$ we find, after some rearrangement,

$$u_{\gamma} = \frac{t_1^{*2}\,\widetilde{G}_{\overline{\gamma}}\,(1 - t_2^*\,\widetilde{G}_{\overline{\gamma}})}{(1 - t_2^*\,\widetilde{G}_{\gamma} - t_2^*\,\widetilde{G}_{\overline{\gamma}})^2} + \frac{t_2^{*2}\,\widetilde{G}_{\gamma}}{1 - t_2^*\,\widetilde{G}_{\gamma}} = \tilde{z} - \epsilon_{\gamma} - \widetilde{G}_{\gamma}^{-1}\,, \quad (32)$$

$$w_{\gamma} = \overline{w}_{\gamma} = \frac{1}{\sqrt{K}}\frac{t_1^* t_2^*\,\widetilde{G}_{\overline{\gamma}}}{1 - t_2^*\,\widetilde{G}_{\gamma} - t_2^*\,\widetilde{G}_{\overline{\gamma}}}\,, \qquad\qquad v_{\gamma} = \frac{1}{K}\frac{t_2^{*2}\,\widetilde{G}_{\overline{\gamma}}}{1 - t_2^*\,\widetilde{G}_{\overline{\gamma}}}\,. \quad (33)$$

For given $\tilde{z}, \epsilon_{\mathrm{A}}, \epsilon_{\mathrm{B}}$, Eq. (32) is a system of two symmetric equations for $\widetilde{G}_{\mathrm{A}}, \widetilde{G}_{\mathrm{B}}$ and we denote the appropriate solution by $\widetilde{G}_{\gamma} = f(\tilde{z}, \epsilon_{\gamma}, \epsilon_{\overline{\gamma}})$; note that this function does not depend explicitly on K. Inserting Eqs. (32)-(33) into (24) we can then express the local Green function as

$$G_{\gamma}(z)^{-1} = \widetilde{G}_{\gamma}^{-1} - \frac{1}{K}R(\widetilde{G}_{\gamma}, \widetilde{G}_{\overline{\gamma}})\,, \qquad\qquad \widetilde{G}_{\gamma} = f(z + \tfrac{t_2^*}{K}, \epsilon_{\gamma}, \epsilon_{\overline{\gamma}})\,, \quad (34)$$

$$R(\widetilde{G}_{\gamma}, \widetilde{G}_{\overline{\gamma}}) = \frac{t_1^{*2}\,\widetilde{G}_{\overline{\gamma}}\,(1 - t_2^*\,\widetilde{G}_{\overline{\gamma}})}{(1 - t_2^*\,\widetilde{G}_{\gamma} - t_2^*\,\widetilde{G}_{\overline{\gamma}})^2(1 - pt_2^*\,\widetilde{G}_{\overline{\gamma}})} + \frac{t_2^*}{1 - t_2^*\,\widetilde{G}_{\gamma}}\,, \quad (35)$$

where again $p = Z/K$. Taking the limit $K \to \infty$ in Eq. (34) we find that $G_{\gamma}^{\infty}(z) = f(z, \epsilon_{\gamma}, \epsilon_{\overline{\gamma}})$, and also $\lim_{K\to\infty} \widehat{G}_{\gamma}(z) = \widehat{G}_{\gamma}^{\infty}(z)$ [Eq. (13)]. This leads us to the remarkable conclusion that *the local Green function $G_{\gamma}(z)$ for arbitrary K is a rational function of the local Green functions $G_{\gamma}^{\infty}(z)$ for infinite K,*

$$G_{\gamma}(z) = \left[G_{\gamma}^{\infty}(z + \tfrac{t_2^*}{K})^{-1} - \frac{1}{K}R\big(G_{\gamma}^{\infty}(z + \tfrac{t_2^*}{K}), G_{\overline{\gamma}}^{\infty}(z + \tfrac{t_2^*}{K})\big)\right]^{-1}. \quad (36)$$

The function G_{γ}^{∞} is determined by Eq. (32). However, this is clearly the same implicit equation that was obtained in (10) and (15), thus confirming the RPE calculation of the previous section. The function $G_{\gamma}^{\infty}(z)$ is obtained in the next section.

Finally we note that the unexpected relation (36) can be checked for only NN hopping,

$$g_\gamma(z) = \left[g_\gamma^\infty(z)^{-1} - \frac{t_1^{*2}}{K} g_{\bar\gamma}^\infty(z) \right]^{-1}, \qquad\qquad (t_2 = 0) \qquad (37)$$

which is indeed fulfilled by the results (6) for this case.

4 Topological approach

4.1 Operator identities for hopping Hamiltonians

Recently a topological approach to the tight-binding spectrum of H_{kin} on the Bethe lattice was developed [14], which we will extend to the case of additional A-B on-site energies H_{loc} here.

We begin with a short review of the method of [14]. Unlike crystal lattices, the (infinite) Bethe lattice has the property that the number of paths between two lattice sites i and j which consist of n NN steps depends only on the topological distance $d_{i,j}$, but not on the relative orientation of i and j. This "distance regularity" entails polynomial relations [37] among the tight-binding Hamiltonians H_d. For the Bethe lattice they are given by [14]

$$U_n(\tilde H_1/2) = \sum_{s=0}^{\lfloor n/2 \rfloor} \frac{\tilde H_{n-2s}}{K^s}, \qquad\qquad \tilde H_d = U_d(\tilde H_1/2) - \frac{1}{K} U_{d-2}(\tilde H_1/2), \quad (d \geq 2) \quad (38)$$

where $U_n(x)$ are the Chebychev polynomials of the second kind [38]. Similar relations involving the Hermite polynomials hold for the infinite-dimensional hypercubic lattice [26,39]. By contrast, Eq. (38) is valid for any K, including the one-dimensional chain ($K = 1$) as well as the limit $K \to \infty$. These relations can also be expressed by means of the generating function

$$\frac{1 - x^2}{1 - xH_1 + Kx^2} = \sum_{d=0}^\infty H_d \, x^d, \qquad\qquad \frac{1 - x^2/K}{1 - x\tilde H_1 + x^2} = \sum_{d=0}^\infty \tilde H_d \, x^d. \qquad (39)$$

From these operator identities one concludes that for the Bethe lattice the eigenstates of any hopping Hamiltonian (1) are the same as those of $\tilde H_1$, and its eigenvalues $\epsilon(\lambda)$ can be expressed as a function of the eigenvalues λ of $\tilde H_1$. The calculation of spectral properties, such as the density of states [14] from this effective dispersion $\epsilon(\lambda)$ is then straightforward. The method works well for arbitrary hopping t_d since no explicit enumerations are required.

We now incorporate the effect of alternating on-site energies [Eq. (2)],

$$H_{\mathrm{loc}} = \sum_{\gamma=\mathrm{A,B}} \epsilon_\gamma \sum_{i \in \gamma} |i\rangle\langle i| = \bar\epsilon + \epsilon V, \qquad V = \sum_i (-1)^i |i\rangle\langle i|, \qquad \frac{\epsilon_\mathrm{A} \pm \epsilon_\mathrm{B}}{2} =: \begin{cases} \bar\epsilon \\ \epsilon \end{cases}, \qquad (40)$$

where $(-1)^i = \pm 1$ for $i \in \mathrm{A, B}$, e.g., $(-1)^i = (-1)^{d_{i,j}}$ for some fixed site $j \in \mathrm{A}$. Since the operators H_{2d} (H_{2d+1}) connect the same (different) sublattices they commute (anticommute) with V, respectively,

$$VH_d - (-1)^d H_d V = 0, \qquad\qquad VH_1^n - (-1)^n H_1^n V = 0, \qquad (41)$$

where the second equation follows from the polynomial relations (38) between H_d and H_1^n. Together with $V^2 = 1$ we immediately obtain the useful new operator identity

$$(\alpha V + \beta H_1)^{2n} = (\alpha^2 + \beta^2 H_1^2)^n, \qquad\qquad n = 0, 1, 2, \ldots. \qquad (42)$$

for arbitrary constants α, β. This identity makes it possible to reduce resolvent operators involving V and H_1 to simpler expressions.

As a simple application let us consider only NN hopping (6). We find by straightforward series expansion and partial fraction decomposition

$$\frac{1}{z - h} = \frac{z - \bar{\epsilon} + \epsilon V + t_1^* \tilde{H}_1}{(z - \bar{\epsilon})^2 - (\epsilon^2 + t_1^{*2} \tilde{H}_1^2)} = \frac{1}{2} \sum_{s = \pm 1} \left(1 + \frac{z - \bar{\epsilon} + \epsilon V}{s \sqrt{x}} \right) \frac{1}{s \sqrt{x} - t_1^* \tilde{H}_1} , \quad (43)$$

again with $x = (z - \epsilon_A)(z - \epsilon_B)$. We therefore conclude that for NN hopping, surprisingly, any Green function for $\epsilon_A \neq \epsilon_B$ can be written as a linear combination of two Green functions for the homogeneous case, $\epsilon_A = \epsilon_B$, at other arguments.

4.2 Results for t_1-t_2 hopping

For t_1-t_2 hopping [Eq. (4)] there are now two possible routes to the local Green function $G_\gamma(z)$ for arbitrary K. On one hand, according to Eq. (36) of the previous section, $G_\gamma(z)$ is determined by $G_\gamma^\infty(z)$ alone. The latter was already obtained in [14] from the operator identity (39) for the homogeneous case, together with a diagonalization of the 2x2 sublattice problem. This gave

$$G_\gamma^\infty(z) = \frac{1}{2t_2^*} + \frac{1}{2(\lambda_2^2 - \lambda_1^2)t_2^{*2}} \sum_{i=1}^{2} \frac{(-1)^i [z_{\bar{\gamma}} - (\lambda_i^2 - 1)t_2^*]\sqrt{\lambda_i - 2}\sqrt{\lambda_i + 2}}{\lambda_i} , \quad (44a)$$

$$\lambda_{1,2} = \sqrt{\mathcal{A} \pm \sqrt{\mathcal{A}^2 - \mathcal{B}}}, \quad \mathcal{A} = 1 + \frac{(z_A - z_B)t_2^* + t_1^{*2}}{2t_2^{*2}} , \quad \mathcal{B} = \left[\frac{z_A}{t_2^*} + 1 \right] \left[\frac{z_B}{t_2^*} + 1 \right], \quad (44b)$$

where $z_\gamma = z - \epsilon_\gamma$ and all square roots are given by their principal branches. While $G_\gamma(z)$ is given explicitly by Eqs. (36) and (44), we note that this approach would be less promising for hopping beyond NNN.

On the other hand we may directly use the operator identities (38) and (42), which provide the relation $\tilde{H}_2 = \tilde{H}_1^2 - p = (vV + \tilde{H}_1)^2 - v^2 - p$, with v arbitrary and $p = Z/K$. This gives us

$$H = H_{\text{loc}} + t_1^* \tilde{H}_1 + t_2^* \tilde{H}_2 = \bar{\epsilon} - t_2^* (p + v^2) + t_1^* (vV + \tilde{H}_1) + t_2^* (vV + \tilde{H}_1)^2 , \quad (45)$$

with $v = \epsilon/t_1^*$. Performing the partial fraction decomposition for the resolvent we arrive at

$$\frac{1}{z - H} = \frac{\xi_1 + \xi_2}{\xi_1 - \xi_2} \sum_{k=1}^{2} \frac{(-1)^k}{\xi_k + \bar{\epsilon} - h} , \qquad G_\gamma(z) = \frac{\xi_1 + \xi_2}{\xi_1 - \xi_2} \sum_{k=1}^{2} (-1)^k g_\gamma(\xi_k + \bar{\epsilon}) , \quad (46a)$$

$$\xi_{1,2} = \frac{-t_1^{*2} \pm \sqrt{t_1^{*4} + 4t_1^{*2} t_2^* (z - \bar{\epsilon}) + 4t_2^{*2} (\epsilon^2 + p t_1^{*2})}}{2t_2^*} , \quad (46b)$$

where $g_\gamma(z)$ again denotes the local Green function (6) for only NN hopping. We note that this remarkably short route to $G_\gamma(z)$ is straightforward to carry out also for hopping *beyond NNN*, as well as for off-diagonal Green functions.

5 Results for the local Green function

Using the results of the previous sections, i.e., Eqs. (36) and (44), or Eqs. (46) and (6), the local Green function is now available for arbitrary t_1-t_2 hopping and on-site energies $\epsilon_{A,B}$ on the Bethe lattice for finite or infinite coordination number.
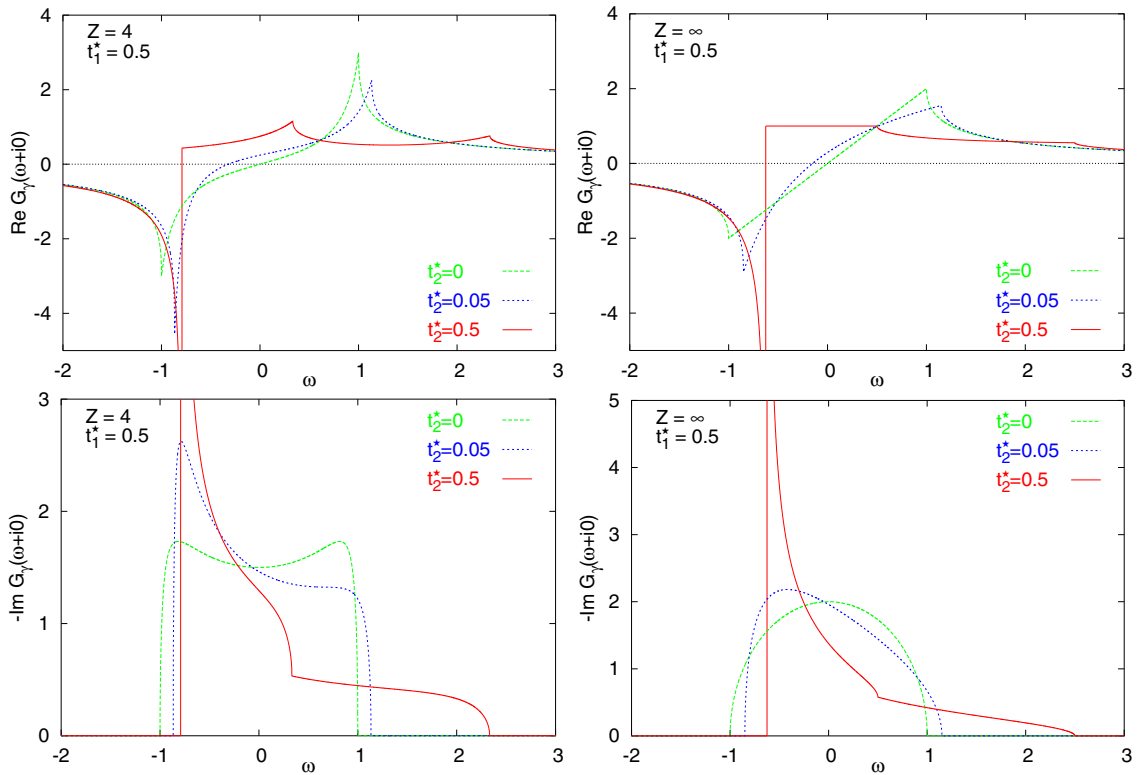
Fig. 5 Local Green function $G_\gamma(\omega + i0)$ for the Bethe lattice with $\epsilon_A = \epsilon_B = 0$, $t_1^* = 0.5$, and $t_2^*/t_1^* = 0, \frac{1}{10}, 1$. Left column: $Z = 4$. Right column: $Z = \infty$. Vertical lines mark divergences.

In Figs. 5–7 we consider both $Z = 4$ and $Z = \infty$ and compare the unfrustrated case ($t_2^* = 0$) to weak frustration ($t_2^* = t_1^*/10$) and strong frustration ($t_2^* = t_1^*$). The homogeneous case, $\epsilon_A = \epsilon_B$, is shown in Fig. 5, whereas we chose $\epsilon_A - \epsilon_B = 2t_1^*$ in Figs. 6 and 7.

From these spectra several effects of frustration may be observed. Beginning with the homogeneous case (Fig. 5) the imaginary part of the Green function, i.e., the density of states, is no longer symmetric if $t_2^* \neq 0$, as noted in Sect. 2. This is the expected generic behavior for a bipartite lattice with hopping between the same sublattices. Furthermore, as discussed already in [14], a square-root singularity at one band edge develops for large enough $|t_2^*|$. For strong frustration one notices the appearance of several additional cusps in both real and imaginary part of the Green function, as well as an increase in bandwidth. It is also apparent that in the limit $Z = \infty$ the Green function loses some of its features. In this case its real part is linear or even flat in part of the band.

These characteristics persist for the case $\epsilon_A \neq \epsilon_B$ (Figs. 6 and 7). In addition the symmetry $G_\gamma(z) = G_{\bar\gamma}(-z)$ is absent for $t_2^* \neq 0$. For strong frustration more van-Hove singularities appear. We also note that the band gap, which is present for only NN hopping due to the alternating on-site energies, is closed for large enough NNN hopping.

In summary, the Green function for t_1-t_2 hopping shows several qualitatively new properties, which are likely to have an impact also on its behavior in interacting many-body or disordered systems, in particular for site-diagonal disorder.
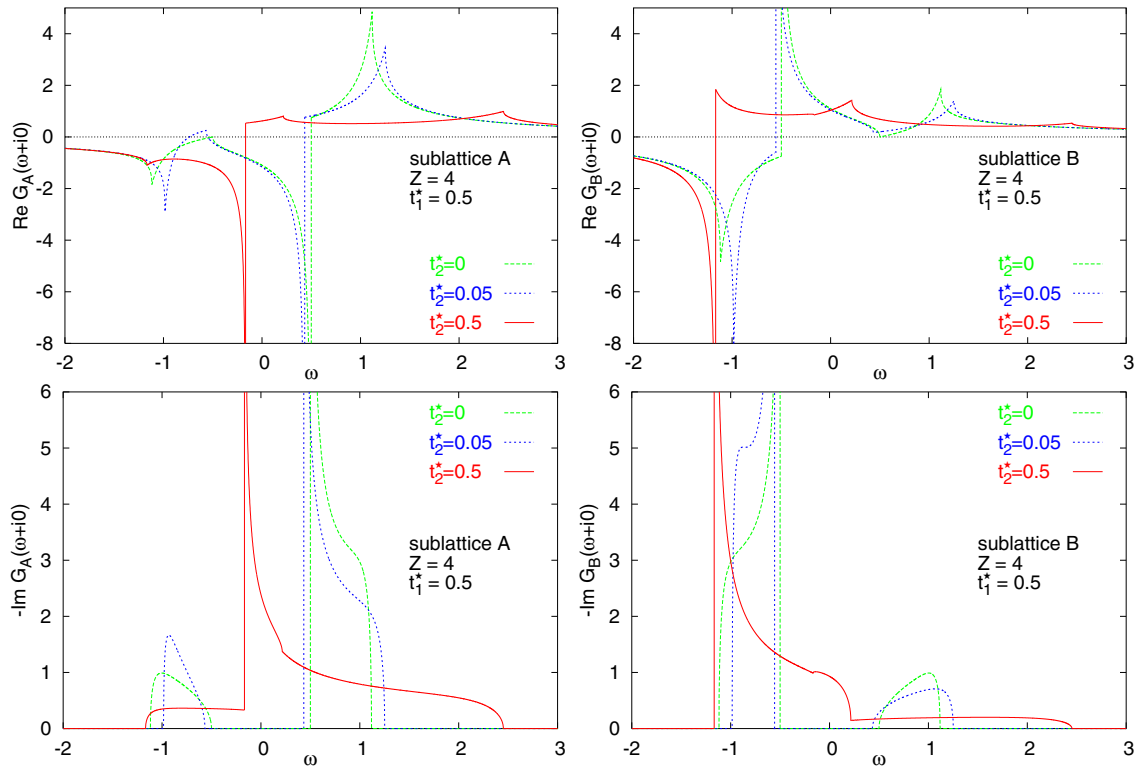
Fig. 6   Local Green function $G_\gamma(\omega+i0)$ for the Bethe lattice with $Z = 4$, $\epsilon_A = -\epsilon_B = t_1^* = 0.5$ and $t_2^*/t_1^* = 0, \frac{1}{10}, 1$. Left column: Local Green function for sublattice A, $G_A(\omega + i0)$, which for $t_2^* = 0$ also appears in [11]. Right column: Local Green function for sublattice B, $G_B(\omega+i0)$; note the small cusp at $\omega = -0.167$. Vertical lines mark divergences.

6   Conclusion

Due to the special topology of the Bethe lattice, the calculation of the Green function of a quantum-mechanical particle for hopping beyond nearest neighbors seemed untractable so far. In this paper we presented the derivation of an explicit expression for the local Green function for t_1-t_2 hopping and sublattice-dependent on-site energies ϵ_A, ϵ_B for arbitrary coordination number Z, employing a set of complementary analytical techniques. Implicit equations for G_γ^∞ were derived by RPE. They also follow from a path integral approach, which furthermore yielded the local Green function G_γ for arbitrary Z as a rational function of G_γ^∞. It should be noted that such a functional relation between Green functions at different Z is quite unexpected and to our knowledge does not occur for any other lattice. From a topological approach explicit expressions for G_γ and G_γ^∞ were obtained in terms of the Green function g_γ for only NN hopping. We found that NNN hopping makes the density of states asymmetric and may induce additional van-Hove singularities, increase the total bandwidth, and close gaps that were opened by alternating on-site energies. From the experience of these results we conclude that it will be worthwhile to investigate the effects which hopping beyond nearest neighbors has on the physics of interacting many-body and disordered systems on the Bethe lattice.
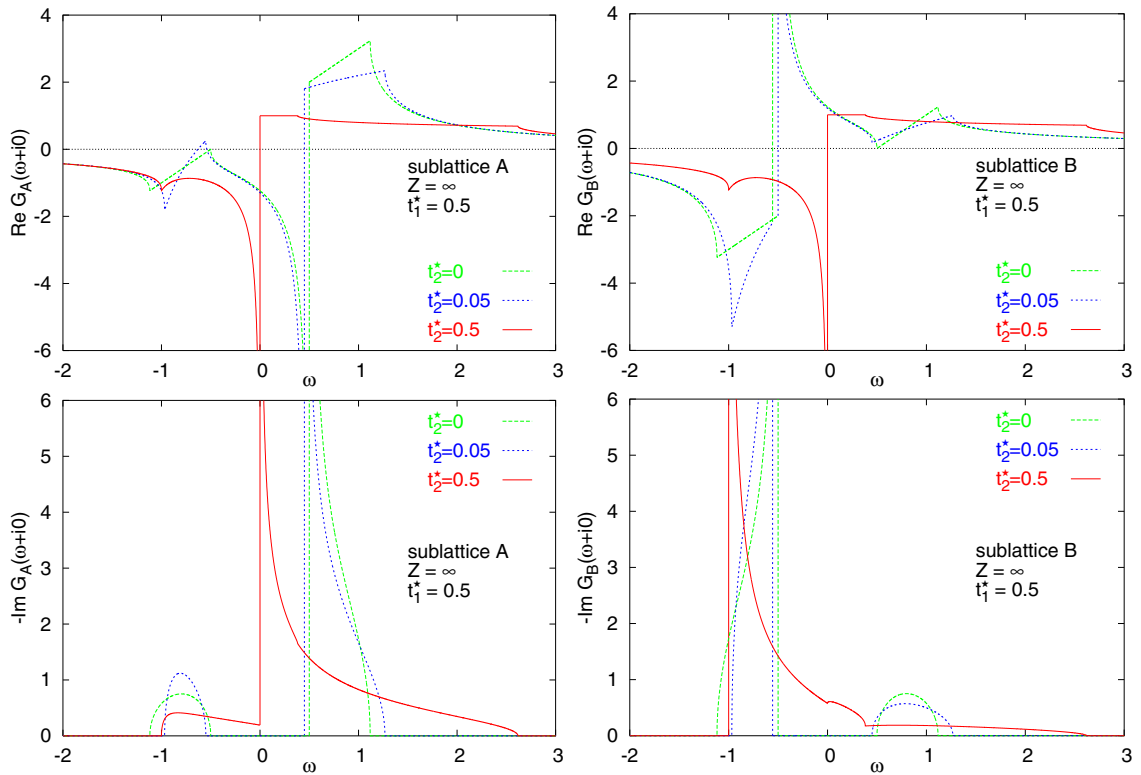
Fig. 7   Same as Fig. 6, but for $Z = \infty$.

References

[1] H. A. Bethe, Proc. R. Soc. London, Ser. A **150**, 552 (1935).

[2] R. J. Baxter, Exactly solved models in statistical mechanics (Academic, London, 1982).

[3] R. Abou-Chacra, D. J. Thouless, and P. W. Anderson, J. Phys. C: Solid State Phys. **6**, 1734 (1973); R. Abou-Chacra and D. J. Thouless, J. Phys. C: Solid State Phys. **7**, 65 (1974).

[4] A. D. Mirlin and Y. V. Fyodorov, Nucl. Phys B **366**, 507 (1991); Phys. Rev. Lett. **72**, 526 (1994); J. Phys. (France) **4**, 655 (1994).

[5] K. Efetov, Supersymmetry in disorder and chaos (Cambridge University Press, Cambridge, 1997).

[6] M. R. Zirnbauer, Phys. Rev. B **34**, 6394 (1986).

[7] D. Weaire and M. F. Thorpe, Phys. Rev. B **4**, 2508 (1971); M. F. Thorpe and D. Weaire, Phys. Rev. B **4**, 3518 (1971); M. F. Thorpe, D. Weaire, and R. Alben, Phys. Rev. B **7**, 3777 (1973).

[8] N. Mingo and L. Yang, Phys. Rev. B **68**, 245406 (2003).

[9] W. F. Brinkman and T. M. Rice, Phys. Rev. B **2**, 1324 (1970).

[10] M. Chen, L. Onsager, J. Bonner, and J. Nagle, J. Chem. Phys. **60**, 405 (1974).

[11] E. N. Economou, Green's Functions in Quantum Physics (Springer, Berlin, 1979).

[12] M. F. Thorpe, in: Excitations in Disordered Systems, edited by M. F. Thorpe (Plenum, New York, 1981), pp. 85–107.

[13] G. D. Mahan, Phys. Rev. B **63**, 155110 (2001).

[14] M. Eckstein, M. Kollar, K. Byczuk, and D. Vollhardt, Phys. Rev. B **71**, 235119 (2005).

[15] W. Metzner and D. Vollhardt, Phys. Rev. Lett. **62**, 324 (1989).

[16] A. Georges and G. Kotliar, Phys. Rev. B **45**, 6479 (1992).

[17] M. Jarrell, Phys. Rev. Lett. **69**, 168 (1992).

[18] D. Vollhardt, in: Correlated Electron Systems, edited by V. J. Emery, World Scientific (Singapore, 1993), p. 57.

[19] Th. Pruschke, M. Jarrell, and J. K. Freericks, Adv. Phys. **44**, 187 (1995).

[20] For a comprehensive review see A. Georges, G. Kotliar, W. Krauth, and M. J. Rozenberg, Rev. Mod. Phys. **68**, 13 (1996).

[21] G. Kotliar and D. Vollhardt, Physics Today **57**, No. 3 (March), 53 (2004).

[22] R. Bulla, Phys. Rev. Lett. **83**, 136 (1999).

[23] M. J. Rozenberg, R. Chitra, and G. Kotliar, Phys. Rev. Lett. **83**, 3498 (1999).

[24] J. Joo and V. Oudovenko, Phys. Rev. B **64**, 193102 (2001).

[25] R. Bulla, T. A. Costi, and D. Vollhardt, Phys. Rev. B **64**, 045103 (2001).

[26] N. Blümer, Ph. D. thesis, Universität Augsburg, 2002; N. Blümer and E. Kalinowski, Phys. Rev. B **71**, 195102 (2005).

[27] M. J. Rozenberg, X. Y. Zhang, and G. Kotliar, Phys. Rev. Lett. **69**, 1236 (1992); M. J. Rozenberg, G. Kotliar, and X. Y. Zhang, Phys. Rev. B **49**, 10181 (1994).

[28] M. J. Rozenberg, G. Kotliar, H. Kajueter, G. A. Thomas, D. H. Rapkine, J. M. Honig, and P. Metcalf, Phys. Rev. Lett. **75**, 105 (1995).

[29] R. Chitra and G. Kotliar, Phys. Rev. Lett. **83**, 2386 (1999).

[30] R. Zitzler, N.-H. Tong, Th. Pruschke, and R. Bulla, Phys. Rev. Lett. **93**, 016406 (2004).

[31] J. Wahle, N. Blümer, J. Schlipf, K. Held, and D. Vollhardt, Phys. Rev. B **58**, 12749 (1998).

[32] S. Daul and R. M. Noack, Z. Phys. B **103**, 293 (1997); Phys. Rev. B **58**, 2635 (1998).

[33] D. Vollhardt, N. Blümer, K. Held, and M. Kollar, in: Band-Ferromagnetism: Ground-State and Finite-Temperature Phenomena, edited by K. Baberschke, M. Donath, and W. Nolting, Lecture Notes in Physics, Vol. 580 (Springer, Heidelberg, 2001), p. 191.

[34] J. W. Negele and H. Orland, Quantum Many-Particle Systems (Addison-Wesley, Redwood City, 1988).

[35] R. Vlaming and D. Vollhardt, Phys. Rev. B **45**, 4637-4649 (1992).

[36] M. H. Radke de Cuba, Ph. D. thesis, RWTH Aachen, 2002.

[37] M. A. Fiol, Discrete Math. **246**, 111 (2002).

[38] Pocketbook of mathematical functions, edited by M. Abramowitz and I. A. Stegun (Harry Deutsch, Thun, 1984).

[39] N. Blümer and P. G. J. van Dongen, in: Concepts in Electron Correlation, edited by A. C. Hewson and V. Zlatic, NATO Science Series (Kluwer, Dordrecht 2003), cond-mat/0303204.